STRUCTURE OF UNDEREXPANDED JET FROM RECTANGULAR NOZZLE

Seiji Tsutsumi
The University of Tokyo, Dept. of Aeronautics and Astronautics

Keywords: *underexpanded jet, rectangular nozzle, linear aerospike engine, SSTO*

Abstract

Structure of underexpanded jets from the square exit nozzle with the exit Mach number of 2.2 was investigated numerically. The nozzle represents one of the clustered combustors of a linear aerospike engine. From the results, it was revealed that the shock structure is composed of three shock waves. One is the recompression shock waves at the corners of the nozzle exit. Second is also the recompression shock waves appearing at the downstream of the symmetry planes. These recompression shock waves are formed following the overexpanded regions formed by the interaction of the Prandtle-Meyer expansion fans emanating from the neighboring nozzle edges. Third is the intercepting shock waves identical with the shock wave observed in two-dimensional underexpanded jets. The correlation between the shock structure and jet boundary expansion was investigated. It was clarified that the jet boundary around the symmetry planes expands outward two-dimensionally, while the jet around the corners turns inward through the recompression shock waves at the corners and the intercepting shock waves. As a result, cross-sectional jet shape becomes a cross-like shape. When the pressure ratio is lower, the expansion fans and the shock waves are not so strong that the cross-sectional jet shape is not transformed so much. On the other hand, for the higher pressure ratio, the recompressoin shock wave at the corners and the intercepting shock wave spread wider in the flow field. Futhermore, the generation point of the intercepting shock wave moves upstream. Therefore, cross-sectional jet shape becomes a diamond-like shape, while only the narrow regions of the jet around the symmetry planes expand outward two-dimensionally.

Nomenclature

f	scalar quantity
M	Mach number
P	pressure
$\mathbf{U}$	velocity vector
X	axial distance from nozzle exit plane
κ	specific heat ratio
D	diameter
NPR	total pressure ratio, $= P_o/P_a$
NPR_e	exit static pressure ratio, $= P_e/P_a$

Subscripts

a	ambient
e	nozzle exit plane
$\mathbf{n}$	unit normal vector
t	throat
o	nozzle inlet stagnation

1 Introduction

Single Stage To Orbit (SSTO) is believed to reduce the space transportation cost and promote our space activities. In order to realize a SSTO, one of the key issues is the development of an efficient propulsion system. A linear aerospike engine (Fig.1) is one of the prominent candidates among the propulsion systems proposed today. This engine has two nozzle. One is an internal nozzle composed of a combustion chamber

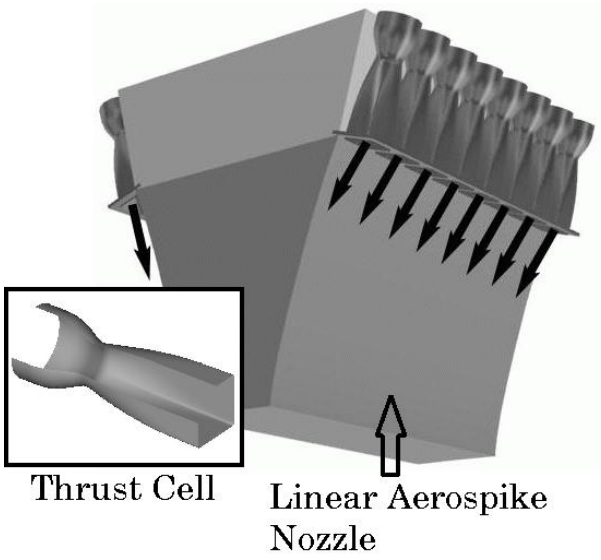

Fig. 1 Linear Aerospike Engine

and a conventional bell-type nozzle. The other is an external nozzle, called linear aerospike nozzle. Unlike a conventional bell-type nozzle, the outer jet boundary on a linear aerospike nozzle exposes to the atmosphere and optimum expanding condition can be maintained over the flight path. Therefore, the nozzle thrust efficiency can be significantly higher, which is the attractive feature for SSTO's propulsion systems. [1, 2]

An internal nozzle is placed on the inlet of a linear aerospike nozzle, and it is divided into several modules, called thrust cells, in order to avoid combustion instabilities and the difficulties related to manufacturing and cooling of the tiny throat gaps. There are several constraints in the design of a thrust cell. Its throat needs to be circular to eliminate excessive heat load. On the other hand, the exit must be rectangular to minimize the losses induced by the gaps between thrust cells and the exhaust flow interactions on a linear aerospike nozzle.

Some investigations have been carried out numerically and experimentally to analyze the interacted flow field on an aerospike nozzle and predict aerospike nozzle performance. Ito and Fujii focused on an axisymmetric aerospike nozzle and discussed the performance of aerospike nozzles numerically. [3] From their results, it was revealed that complicated flow field appear on the aerospike nozzle surface, and the performance deteriorate due to the gaps between the thrust cells. Moreover, Sakamoto et al. constructed and tested 3-clustered combustor for a linear aerospike nozzle with 14.4[kN] nominal thrust. [4] It was observed that the interacted flow field causes high heat load on the aerospike nozzle surface. The interaction of underexpanded jets from thrust cells can be one of the key factors for the development of a linear aerospike engine.

The jets issuing from noncircular nozzles at relatively low pressure ratio have been studied extensively. For expample, they are applied to a passive mixing techniques, noise suppression device and thrust vector control. [5] Teshima studied underexpanded jets from rectangular sonic orifices for high pressure ratios and showed how the jet cross-section develops into the cross-like shape as they go downstream. [6] Expansion fans and shock waves exist in supersonic jets, and they dominate the flow field. However, neither the three-dimensional shock structure nor its correlation with the jet boundary expansion is not clarified yet. Therefore, the objective of the current study is to reveal the flow structure of underexpanded jets from a nozzle with rectangular exit.

The nozzle tested in this study has a square exit with M_e of 2.2. General aspect of the flow field for NPR_e=2.5 is discussed based on the numerical results. The flow structures for different pressure ratios are also investigated.

2 Numerical Approach

2.1 Numerical Method

The governing equations employed here are the Reynolds-averaged three-dimensional Navier-Stokes equations. Physical properties are normalized by density, sound speed and viscous coefficient at the nozzle inlet stagnation condition. Length is normalized by the diameter of the throat.

Numerical fluxes for the convective terms are evaluated by the Simple High-resolution Upwind

Scheme (SHUS) [7], and it is extended to higher-order (third order) by the MUSCL interpolation based on the primitive variables. Since steady-state solutions are only considered, the Lower-Upper Alternating Direction Implicit (LU-ADI) algorithm is employed for time integration. [8]

Under symmetry assumption, a quarter of the flow field is only calculated to analyze the steady-state jet structure of the first shock cell. The computational domain used in the simulation is shown in Fig.2. Fine domain is located near the edge of the nozzle exit plane to resolve the rapid expansion of the jet. Large difference in the grid spacing between the fine domain and the coarse background domain causes the mismatch of physical properties at the boundary, therefore a middle spacing domain is placed between the two. Total number of the grid is about 5 million at most. The Fortified Solution Algorithm is employed to transfer the computed physical data between each domains. [9]

The simulations is executed on the HITACHI SR8000/MPP at the University of Tokyo, and the computational code is parallelized by hybrid MPI/OpenMP implementation.

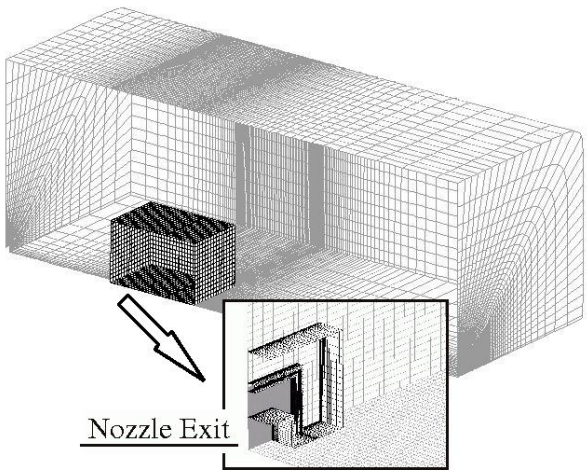

Fig. 2 Computational Domains

2.2 Shock Detection Algorithm using CFD Results

Expansion fans and shock waves can be the key factor to determine the expansion of supersonic jet boundary. Thus, visualization of three-dimensional shock surface is required in this study to analyze the flow field.

There are two types of shock detection algorithms using CFD results. One is based on the Normal Mach Number: M_n which is the Mach number normal to a shock surface.

$$M_n = \vec{M} \cdot \mathbf{n} = \vec{M} \cdot \frac{\nabla f}{|\nabla f|} \tag{1}$$

A shock is considered to be located where the Normal Mach Number exceeds one. [10]

The other method employs the Directional Derivative which is the derivative of a scalar quantity in the direction of the local velocity vector as follows.

$$\delta_1 f = \frac{\mathbf{U}}{|\mathbf{U}|} \cdot \nabla f \tag{2}$$

$$\delta_2 f = \frac{\mathbf{U}}{|\mathbf{U}|} \cdot \nabla (\delta_1 f) \tag{3}$$

The position of a shock wave is assumed to be placed where $\delta_2 f$ is zero while $\delta_1 f$ is non-zero. [11]

The difficulty in the shock detection algorithm using CFD results is how to remove the noise contained in the solutions. Therefore, trial-and-error is required to find the best fitted shock detection algorithms and filtering techniques for the target flow field. In order to filter out physically relevant normal vectors, the filtering technique proposed by Cebral and Löhner was employed in the present study. [10] Absolute value of the local velocity vector was selected as f. When the Directional Derivative is applied, static pressure was chosen as f. Two threshold values were set to find zero-level iso-surface of $\delta_2 f$ and to discard expansion fans by the sign of $\delta_1 f$ respectively.

3 General Aspect of Underexpanded Jet Structure NPR_e=2.5

In this section, general aspect of the underexpanded jet from the square nozzle is discussed. NPR_e=2.5 is selected as an representative case. Figure.3 shows the shock surface painted with the pressure gradient magnitude as a measure of shock strength. The shock surface is found to be classified into four groups(A-D). Firstly, the shock surfaces of group A appear at the four corners of the nozzle exit. Then, group A disappears at the downstream, where the next group of B emerges only around the symmetry planes. The shock surfaces of group B are inclined inward. The third group of C is very complicated. The shock surfaces emerge at both of the symmetry and diagonal planes. Finally, group D expands outward around the symmetry planes.

Figure.4 shows cross-sectional density contours with shock surfaces. The density contours are only displayed where the pitot pressure is higher than a certain threshold, and they show the cross-section of the jet shape. The jet expands outward at the symmetry planes, while the jet does not expand so much around the diagonal planes. As a result, the jet issuing from the square nozzle is deformed to be a cross-like shape. Moreover, at X/D_t=4.2, the jet around the diagonal planes turns inward more, so the cross-like shape becomes more distinct. The underexpanded jet structure observed in Fig.4 has a correlation with the shock wave structure. Therefore, the shock wave structure is investigated, and the correlation between the shock structure and the jet structure is analyzed in the following subsections.

3.1 Shock Wave Structure

Figure.5 shows the density contours at the symmetry and diagonal planes. At the symmetry plane, the oblique shock wave is formed at about X/D_t=2.0 which belongs to the group B. This oblique shock intersects regularly at X/D_t=4.2. Whereas, at the diagonal plane, the shock wave of group A appears just behind the nozzle exit

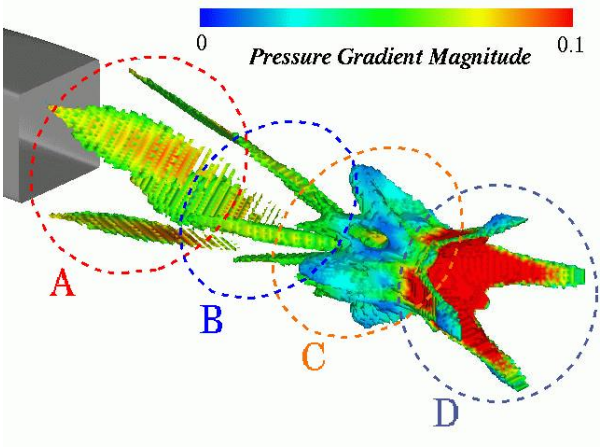

Fig. 3 Shock Surface Painted with Pressure Gradient Magnitude

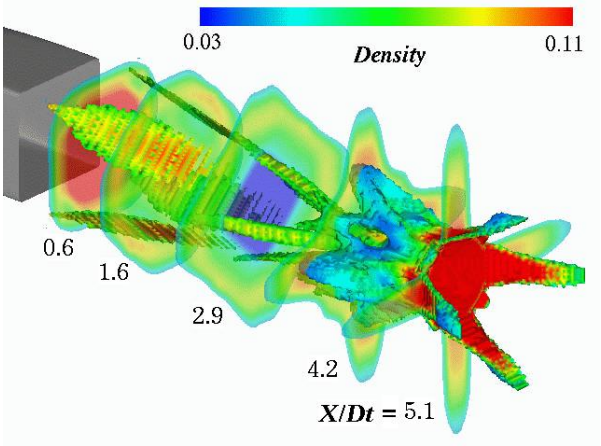

Fig. 4 Shock Surface with Cross-Sectional Density Contour

plane. It is clear that both of these two shock waves are different from the intercepting shock wave observed in two-dimensional planar underexpanded jets, because intercepting shock waves are formed by the reflection of expansion fans from a nozzle lip. Figure.6 shows the static pressure distributions at four cross-sections. The overexpanded regions is observed at the four corners at X/D_t=0.5 and 1.1. The exit shape is square, Prandtl-Meyer expansion fans are generated from the four nozzle edges. The Prandtl-Meyer expansion fans from the neighboring nozzle edges interact with each other at the corner regions, and then the jet of these regions overexpand. The static pressure at these regions is found to be lower than the ambient pressure as shown in

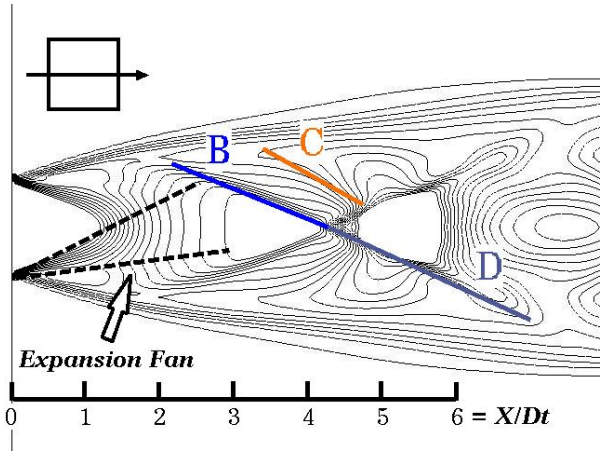

(a) Symmetry Plane

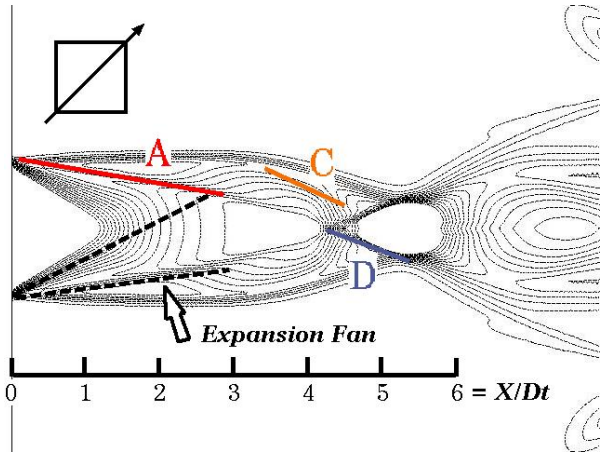

(b) Diagonal Plane

Fig. 5 Schematics of Flow Structure at Symmetry and Diagonal Planes

Fig.6, therefore recompression shock waves are formed to recover the static pressure. The shock waves of group A shown in Fig.3 and 5(b) correspond to this recompression shock wave.

As the jet flows downstream, the overexpanded regions grow larger, and then intersect with each other at X/D_t=1.7, 2.6. Consequently, another recompression shock wave belonging to group B emerges at the symmetry plane.

It is observed from Fig.5 that the generation point of the shock wave of group C is about X/D_t=3.4 at both of the planes. The Mach angle of the head and tail of the expansion waves from the nozzle lip are 27.0[deg] and 7.2[deg] respectively from the Prandtl-Meyer's theory. Roughly speaking, the generation point of the shock waves coincides with the intersection point of head of expansion wave with the jet boundary. Thus the shock waves of group C is the intercepting shock wave.

From Fig.5, the shock wave of group D at the symmetry plane turns out to be the recompression shock wave of group B after the regular intersection. The shock wave of group D at the diagonal plane (Fig.5(b)) also seems to be the recompression shock wave of group A after the regular intersection. However, the strength of the group A between X/D_t=3 and 4.2 is so weak that the present shock detection algorithm did not account the pressure gradient in this region to be shock wave, therefore the shock wave of group A disappears at X/D_t=3 in Fig.3. The expansion fans coming from the nozzle edges meet the shock wave A, which is mainly responsible for its attenuation in this region.

3.2 Correlation between Shock Wave and Jet Boundary

In order to reveal how the jet boundary expands three-dimensionally, firstly, the correlation between the shock waves and the jet boundary is studied at the symmetry and diagonal plane (Fig.5). It is observed that the jet expands outward at the symmetry plane, on the other hand, it does not expand so much at the diagonal plane.

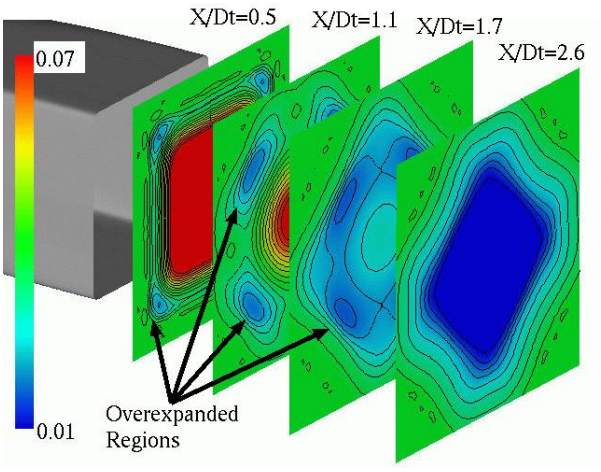

Fig. 6 Cross-Sectional Static Pressure Distributions

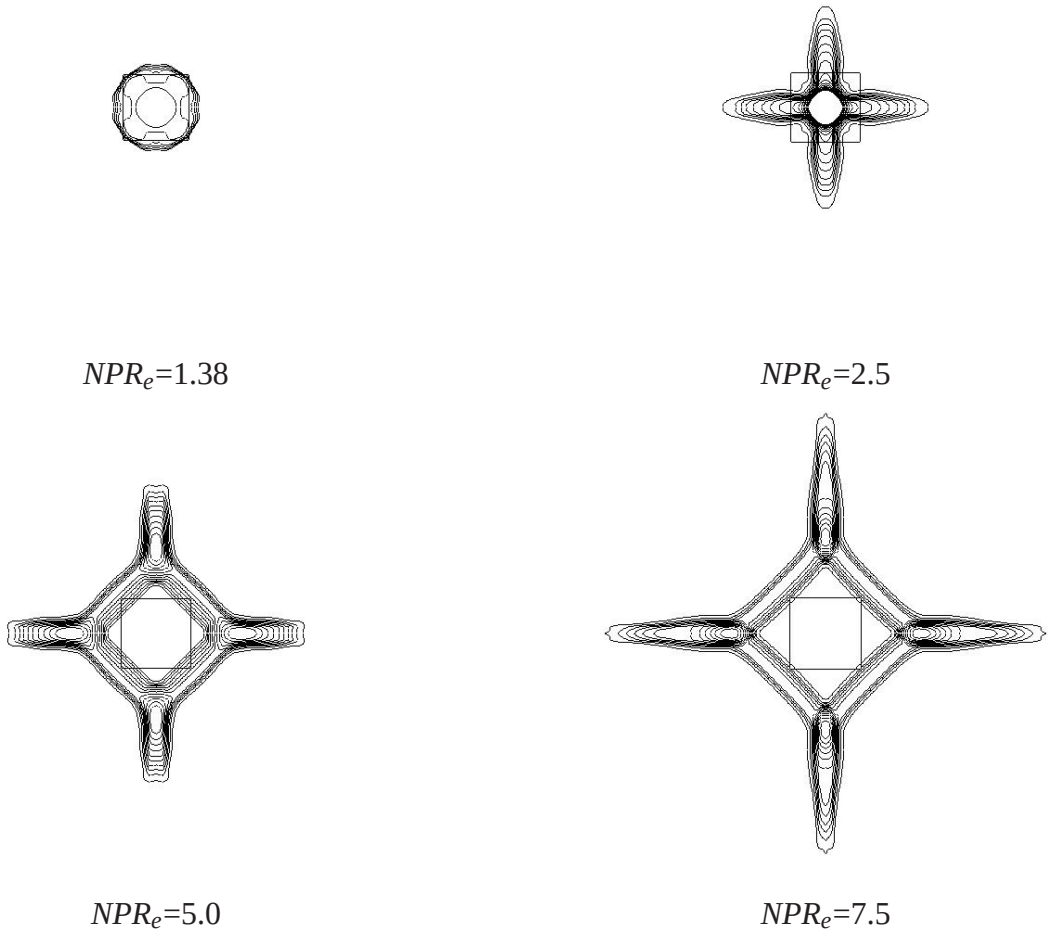

Fig. 7 Comparison of Cross-Sections illustrated with Density Contour

At the symmetry plane, the jet passes through the Prandtl-Meyer expansion fan from the nozzle edge, thus the exit expansion angle of Fig.5(a) agrees with the value calculated from the Prandtl-Meyer's theory, which is 19.9[deg] in this case. On the other hand, the jet boundary at the diagonal plane meets the recompression shock wave just after the expansion fans, therefore it turns inward.

Another recompression shock wave is formed at about X/D_t=2.0 at the symmetry plane. However, Fig.5(a) shows there is almost no effect on the jet boundary, because the streamline of the jet boundary does not go through the recompression shock wave.

At the downstream, the numerical results shown in Fig.5(b) indicates that the jet boundary of the diagonal plane turns inward more at about X/D_t=3. This is because of the intercepting shock wave. This shock also appears at the symmetry plane, however, its effect seems weak. In order to investigate the effect, grid resolution and space accuracy of the present scheme need to be reconsidered.

The recompression shock wave intersects regularly, and then extends to the jet boundary. So the first shock cell ends when the recompression shock wave meets the jet boundary.

The above discussions focus only on the symmetry and diagonal planes, and Fig.4 shows the three-dimensional flow field. Because of the re-

compression shock waves around the nozzle corners, the jet around the diagonal planes turns inward, while around the symmetry planes the jet expands outward two-dimensionally. Thus the cross-section becomes a cross-like shape. At about X/D_t=3.0, the jet passes through the recompression shock waves. At the symmetry plane, however, the jet still expands. On the other hand, at the diagonal plane, the jet turns inward more, and the cross-sections becomes more distinct cross-like shape.

4 Effect of Pressure Ratio

Figure.7 compares cross-sectional jet shapes illustrated with the density contour at four different pressure ratios. It is clear that the jet shape is influenced by the nozzle pressure ratio. For the lowest pressure ratio in this study, NPR_e=1.38, only small deformation can be seen. On the contrary, the cross-like shapes become distinct with the increase of the pressure ratio. In the case of NPR_e=5.0 and 7.5, the cross-sections look like a diamond-like shape. It is also noticeable that the jet expands outward remarkably only at the symmetry planes.

When NPR_e is 1.38, the reason is clear. The strength of the expansion fans and shock waves are not so strong as to transform the jet boundary. On the other hand, for the case of NPR_e=5.0 and 7.5, the strength of the expansion fans and the shock waves alone do not explain the difference in the jet shape. Figure.8 shows the shock surface with the cross-sectional density contours for NPR_e=7.5. In the same manner as Fig.4, the shock surface is painted with the pressure gradient magnitude and the pitot pressure is set for the threshold value to indicate the jet boundary. It is observed that the recompression shock waves are formed at the corners of the nozzle exit and at the symmetry planes. Besides, Fig.8 indicates that the intercepting shock wave is larger than that of NPR_e=2.5 (Fig.4) and covers the flow field between the recompression shock waves at the symmetry planes. Furthermore, it appears more upstream of the Mach intersection point.

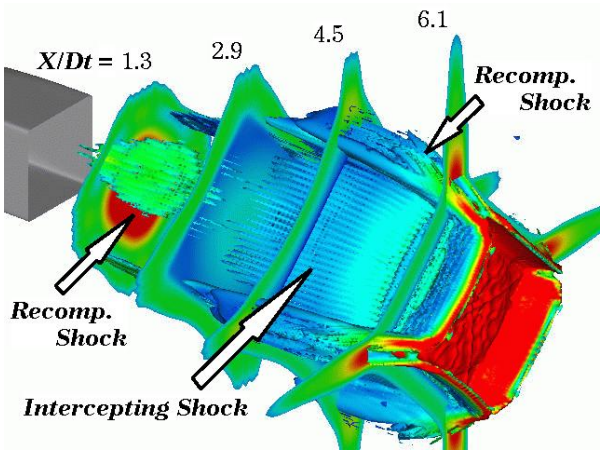

Fig. 8 Shock Surface with Cross-Sectional Density Contour for NPR_e=7.5

The central angle of the expansion fan from the nozzle lip is larger for NPR_e=7.5 than for NPR_e=2.5. From the Prandtl-Meyer's theory, the angle is 38.3[deg] for NPR_e=7.5, while it is 19.9[deg] for NPR_e=2.5. Therefore, the overexpanded region around the corner of the nozzle exit, eventually the recompression shock wave, becomes larger. Moreover, the intercepting shock wave is formed more upstream and spreads wider in the flow field.

Under the influence of the shock structure mentioned above, larger part of the jet turns inward through the recompression shock waves around the corners, while narrow part only around the symmetry planes expands outward two-dimensionally. As the jet flows downstream, the jet boundary other than the symmetry planes turns inward more because of the intercepting shock waves. As a result, cross-sections of the jet becomes a diamond-like shape, whereas narrow part of the jet around the symmetry planes expands outward remarkably.

5 Concluding Remarks

The underexpanded jets from the square exit nozzle representing one of the clustered combustors of the linear aerospike engine was studied numerically. Firstly, the general features of the jet was investigated by using the NPR_e=2.5 case. It was revealed that he three-dimensional shock struc-

ture consists of three shock waves. One is the recompression shock wave generated at the corners of the nozzle exit. The Prandtl-Meyer expansion fans coming from the neighboring vertical and horizontal nozzle edges interacts with each other, and then the flow around there overexpands. Since the static pressure of the overexpanded regions are lower than the ambient pressure, the recompression shock waves are formed following the overexpanded regions at the corners of the nozzle exit. As the jet flows downstream, these overexpanded regions grows larger to intersect with each other at the symmetry planes. Therefore, another recompression shock wave is generated at the symmetry plane which corresponds to the second shock wave. Third one is the intercepting shock wave generated for the same reason as that of two-dimensional planar underexpanded jets.

The three-dimensional shock structure was visualized by the shock detection algorithm, and the correlation between the shock structure and the jet boundary expansion was revealed. The jet around the symmetry planes expands outward two-dimensionally, while the jet around the diagonal planes turns inward through the recompression shock waves and intercepting shock waves. Consequently, cross-sectional jet shape becomes a cross-like shape.

Even if the pressure ratio changes, the shock structure is sill composed of the three shock waves. However, their generation points and the size are different, which transforms cross-sectional jet shape. For the lower pressure ratio, NPR_e=1.38, the strength of the expansion fans and shock waves are not so strong that the cross-sectional jet shape does not change so much. On the other hand, for the higher pressure ratio, NPR_e=5.0 and 7.5, the recompression shock wave around the corner region become larger. Furthermore the intercepting shock wave appears more upstream and spreads wider in the flow field. Therefore, larger part of the jet turns inward and become a diamond-like shape, while narrow part around the symmetry planes expand outward two-dimensionally.

References

[1] Sutton G.P. and Biblarz O. *Rocket Propulsion Elements* Seventh Edition. Wiley-Interscience Publication, 2001

[2] Ruf J.H. and McConnaughey P.K. The Plume Physics behind Aerospike Nozzle Altitude Compensation and Slipstream Effect. AIAA 97-3218, 1997

[3] Ito T. and Fujii K. Flow Field and Performance Analysis of the Simplified Clustered Aerospike Nozzles. AIAA 2001-2861, 2001

[4] Sakamoto, H., Takahashi, M., Sasaki, M., Tomita, T., Kusaka, K. and Tamura, H. An Experimental Study on a 14 kN Linear Aerospike-Nozzle Combustor. AIAA 99-2761, 1999

[5] Gutmark, E.J. and Grinstein, F.F. Flow Control with Noncircular Jets. *Annual Review of Fluid Mechanics*, pp.239-272, 1999

[6] Teshima, K. Two-dimensional Focusing of a Supersonic Free Jet by a Rectangular Orifices. *Physics of Fluids*, Vol.30, pp.1899-1901, 1987

[7] Shima, E. and Jounouchi, T. Role of CFD in Aeronautical Engineering (No. 14) - AUSM type Upwind Schemes -. *Proceedings of the 14th NAL Symposium on Aircraft Computational Aerodynamics*, pp.7-12, 1977

[8] Obayashi, S., Matsushima, K., Fujii, K. and Kuwahara, K. Improvements in Efficiency and Reliability for Navier-Stokes Computations Using the LU-ADI Factorization Algorithm. AIAA 86-0338, 1986

[9] Fujii, K. Unified Zonal Method Based on the Fortified Solution Algorithm. *Journal of Computational Physics*, Vol.118, pp.92-108, 1995

[10] Cebral, J.R. and Löhner, R. Visualization on Unstructured Grids using Geometrical Cuts, Vortex Detection and Shock Surfaces. AIAA 2001-0915, 2001

[11] Pagendarm, H.G. and Seitz, B. An Algorithm for Detection and Visualization of Discontinuities in Scientific Data Fields Applied to Flow Data with Shock Waves. *Scientific Visualization - Advanced Software Techniques* -, Ellis Hortwood, New York, pp.161-177, 1993